Intracellular Microenvironment-Responsive Dendrimer-Like Mesoporous Nanohybrids for Traceable, Effective, and Safe Gene Delivery

*Xin Du, Lin Xiong, Sheng Dai, Freddy Kleitz, and Shi Zhang Qiao**

In order to create advanced functional nanocarriers for efficient gene therapy, novel intracellular microenvironment-sensitive fluorescence label-free nanostructured dendrimer-like silica hybrid nanocarriers are developed for traceable, effective, and safe gene delivery. Dendrimer-like mesoporous silica nanoparticles (DMSNs) with center-radial large pores are covalently modified with short polyethyleneimine (PEI) for efficient gene loading and binding. Autofluorescent and biodegradable PEI (AC-PEI) responsive to the intracellular microenvironment are then coated on the gene-loaded nanoparticles for inhibiting gene leakage from the carriers. Moreover, AC-PEI coating not only endows intracellular microenvironment-responsive gene release property, but also allows monitoring the gene delivery process in the absence of external labelling, owing to the pH- and GSH-responsive autofluorescence and biodegradability of AC-PEI. The resultant nanocarriers show high gene loading capacity, low cytotoxicity, stimuli-responsive gene release, label-free, and simultaneous fluorescence tracking, and high gene silencing capability. Thus, these developed nanocarriers hold substantial and promising potential as effective and safe gene-delivery carriers for future scientific investigation and practical implications in gene therapy.

1. Introduction

Gene therapy is considered as a significant and promising strategy for the treatment of genetic diseases, such as cancer.[1–5] However, successful gene therapy is strongly depending on the development of gene delivery systems since naked nucleic acids can be rapidly degraded in the body by endogenous nucleases, and cannot get across cell membranes. Prerequisites for ideal gene delivery carriers are the capabilities of high gene loading, efficient gene protection, being tissue-friendly and nontoxic, passive or active cell targeting, and effective endosome escape and gene release.[1–5] Recently, mesoporous silica nanoparticles (MSNs) have been proven to be a valuable platform to construct various multiple functional smart drug and/or gene delivery systems owing to their attractive characteristics such as stable structures, large surface areas and pore volumes, tunable pore sizes and particle sizes, easy surface modification and high biocompatibility.[6–20] Compared to other carriers, the porous structures of MSNs not only can encapsulate and protect a relatively large amount of cargoes, but also achieve sustainable or controllable cargo release under physiological conditions.

For MSNs-based gene carriers, the functionalization of organic groups with positive charges (e.g., amine,[10] polyethyleneimine,[11–13] poly L-lysine,[14] polyamidoamine,[15] poly(2-dimethylaminoethyl methacrylate)[16] on the pore surface of the particles is a prerequisite for efficient gene binding through electrostatic interactions. Although gene molecules can successfully be adsorbed into the mesopores for most of the current MSNs-based gene delivery systems, a few gene molecules can still be liberated rapidly in cell culture medium or simulated blood solution due to the preferential adsorption of many negatively charged compounds onto the particles replacing the gene molecules.[17,18] Unexpected gene leakage will cause severe immune response, thus restricting their in vivo application. In addition, efficient gene release from carriers is of great significance to achieve the desired biological functions in the targeted intracellular microenvironment. Therefore, the development of stimuli-responsive gene delivery systems, whereby carrier biodegradation and gene release can be selectively triggered by the specific environment in target sites, is imperative and highly desired for modern gene therapy methods.[19–23]

Although MSNs are considered as biocompatible with low cytotoxicity, reports about their dose-dependent toxic effects on biological systems have leaded to serious concerns over their safety.[24] Therefore, it is essential to improve the gene delivery capacity of MSNs, which implies that the needed therapy effect must be achieved by employing low amount of the silica carriers with negligible toxic effect. From the viewpoint of the carrier size and structure, MSNs with small particle size and large pore size should be the ideal carrier to achieve high gene loading capacity and easy cellular uptake, thus enhancing the

Dr. X. Du, L. Xiong, Prof. S. Dai, Prof. S. Z. Qiao
School of Chemical Engineering
The University of Adelaide
SA 5005, Australia
E-mail: s.qiao@adelaide.edu.au
Prof. F. Kleitz
Department of Chemistry and Centre de
Recherche sur les Matériaux Avancés (CERMA)
Université Laval
Quebec City, QC, G1V 0A6, Canada

DOI: 10.1002/adfm.201402408

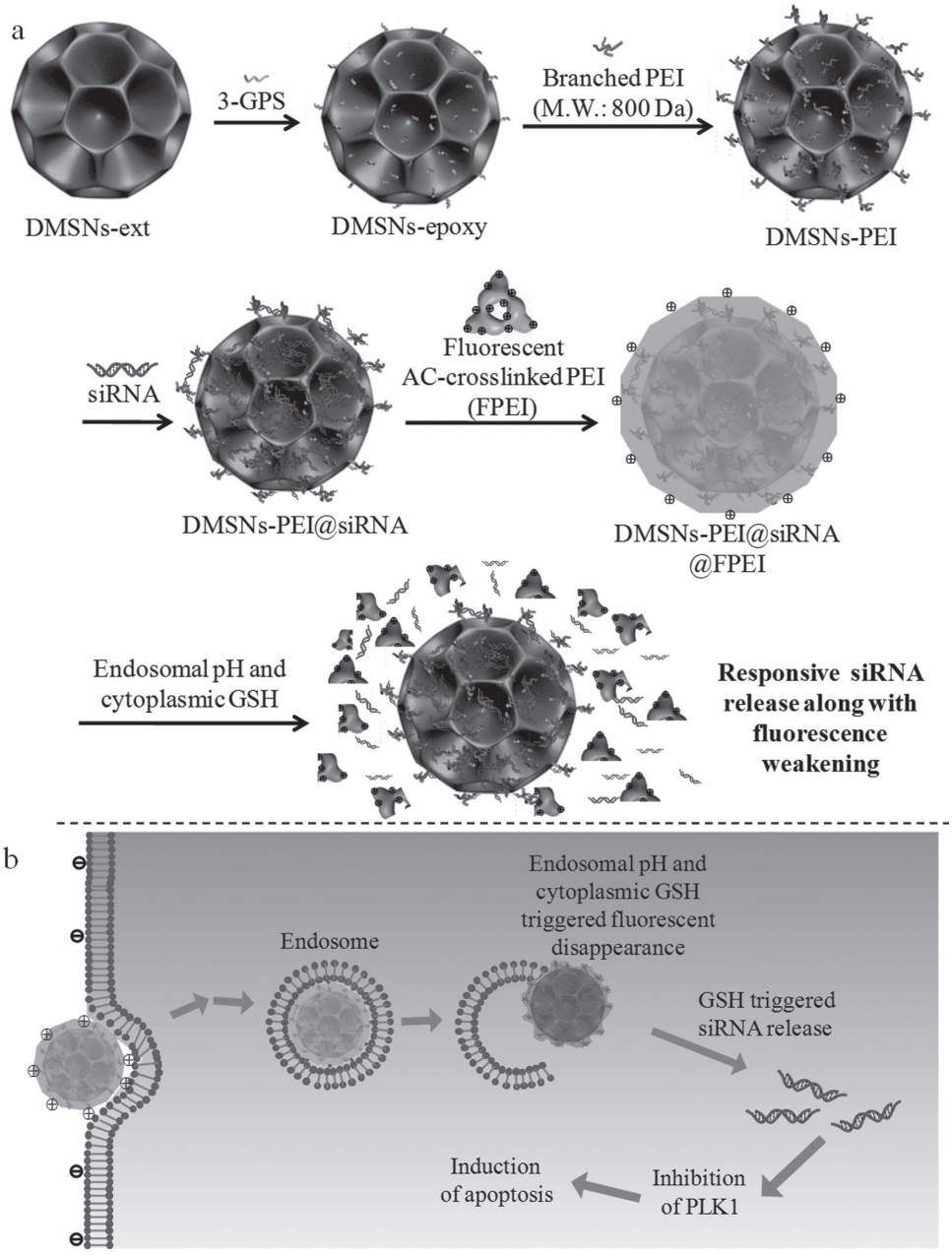

Scheme 1. a) Construction of advanced gene delivery systems (DMSNs-PEI@siRNA@AC-PEI) based on dendrimer-like silica nanoparticles. b) The fluorescent traceable and controlled gene delivery of the delivery systems in cells.

delivery efficiency.[10–18,25,26] However, in most reported works, small (<200 nm) MSNs with small mesopores (2–4 nm) or larger (>200 nm) MSNs with large mesopores (5–20 nm) are employed as platform for gene carrier.[10–18,25,26]

Since gene delivery is an intricate and complicated multiple-step process, fluorescent labelling is always used to monitor the delivery process so as to provide guidance on the optimization of the carrier design and delivery efficiency. In practice, various fluorophores are commonly applied to label gene carriers to obtain detectable fluorescence signals.[10–18] However, the conjugation of fluorescent labels might result in the change of surface charges, wettability, and others effects, to affect further surface modification and functionalization. In addition, the cost, biosafety and disposal of the fluorescent materials are other problems in practical applications. Therefore, auto-fluorescent gene delivery vectors without external fluorophore labelling should be pursued, but the construction of such vectors is still highly challenging.[27–29]

In this study, to address these problems, we developed a novel intracellular microenvironment-sensitive fluorescence label-free nanocarrier system based on nanostructured dendrimer-like silica hybrids for traceable, effective and safe gene delivery. As shown in **Scheme 1**a, small uniform dendrimer-like mesoporous silica nanospheres (DMSNs) with center-radial

large pores are used as the matrix of nanocarriers owing to their unique structures allowing high gene loading. The non-toxic low molecular weight branched polyethyleneimine (PEI, M.W. ≈ 800 Da) are covalently grafted on the pore surface for strong gene binding. Biodegradable and autofluorescent AC-PEI exhibiting an unique intracellular microenvironment-responsive structure, which is synthesized by using acetaldehyde-modified-cystine (acetaldehyde-cystine, AC) to crosslink PEI (M.W. ≈ 800 Da) (Scheme S1, Supporting Information),[30,31] is employed to coat the surface of gene-loaded DMSN particles for inhibiting gene leakage (Scheme 1b).[18] Moreover, the stimuli-responsive fluorescent and degradable properties of AC-PEI toward the endosomal acidic pH and cytoplasmic glutathione (GSH, a tripeptide reducing agent) not only can achieve controlled gene release, but also monitor the gene delivery and release profiles in the absence of external labelling (Scheme 1 and S1).

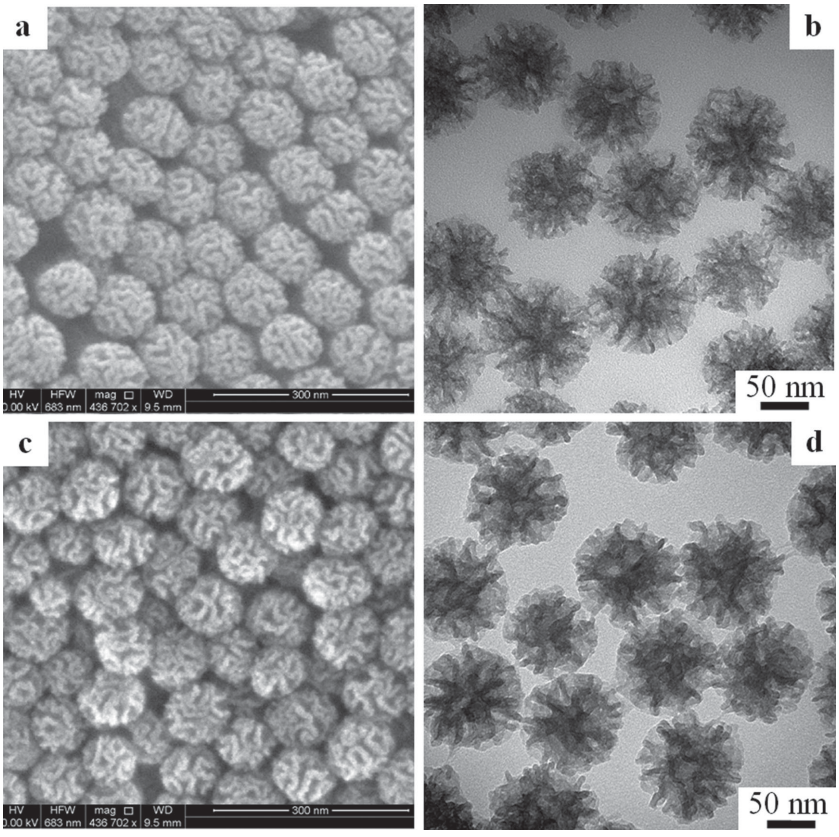

Figure 1. a,c) SEM and b,d) TEM images of a,b) DMSNs-ext and c,d) DMSNs-PEI.

2. Results and Discussion

2.1. Synthesis and Characterization of DMSNs-PEI

Small uniform DMSNs with center-radial large pores were synthesized using hexadecyltrimethylammonium p-toluenesulfonate as the templating surfactant and triethanolamine as the mineralizing agent according to a recently reported method.[32] Scanning electron microscopy (SEM) and transmission electron microscopy (TEM) images in Figure S1, Supporting Information, and **Figure 1**a,b show that the extracted DMSNs (DMSNs-ext) have uniform particle size of 90–120 nm and many center-radial large pores of 8–40 (20 ± 12) nm on the particle surface.

The mesoporosity is further validated by nitrogen adsorption measurements (**Figure 2** and **Table 1**). The adequate particle size together with the unique pore structure makes such DMSNs-ext particles ideally suitable to be used as gene nanocarriers. In order to improve the gene binding affinity of DMSNs-ext nanocarriers, surface modification of highly positive charges was carried out through grafting of non-toxic low molecular weight branched PEI (M.W.: 800) onto DMSNs-ext, as shown in Scheme 1a and S2, Supporting Information. Epoxysilane was firstly grafted onto DMSNs-ext to produce DMSNs-epoxy via alcoholysis reaction. Then, PEI was covalently linked to DMSNs to yield DMSN-PEI through nucleophilic reaction between the nitrogen in the amine group of PEI and the carbon atom of the epoxy ring. After PEI grafting, DMSNs-PEI exhibit a slight decrease of center-radial pore sizes from 8–40 (20 ± 12)

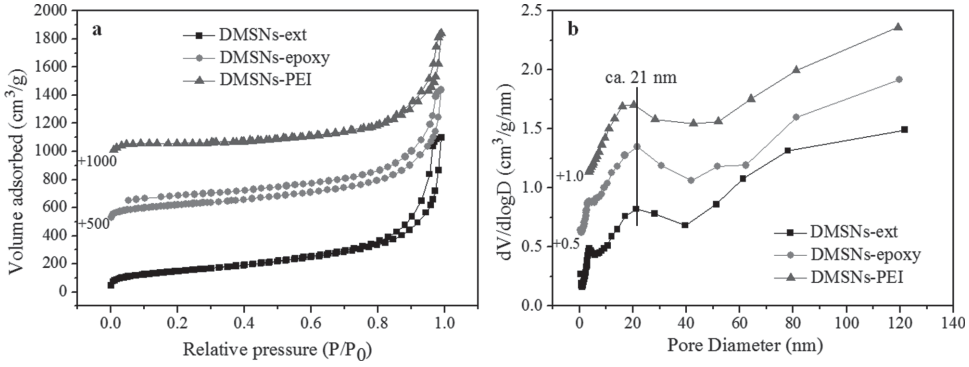

Figure 2. a) N_2 adsorption-desorption isotherms and b) the corresponding BJH pore size distribution curves of DMSNs-ext, DMSNs-epoxy and DMSNs-PEI. The isotherm curves and BJH pore size distribution curves are shifted along y axis for clarity.

Table 1. Physicochemical properties of the synthesized DMSNs obtained from nitrogen sorption isotherms in Figure 2.

Sample	BET surface area (m^2 g^{-1})	Pore size (nm)	Total pore volume (cm^3 g^{-1})
DMSNs-ext	546	21	1.70
DMSNs-epoxy	458	21	1.45
DMSNs-PEI	326	19	1.16

to 6–38 (18 ± 11) nm, but there is no obvious change in the particle size (Figure 1c,d).

The nitrogen adsorption-desorption curves of DMSNs-ext, DMSNs-epoxy and DMSNs-PEI show type-IV behavior, indicating the existence of mesopores (Figure 2a). The corresponding BJH pore size distributions (Figure 2b) obtained from the adsorption branch show a broad peak centered at 21 nm for DMSNs-ext. After grafting of the epoxy groups on the surface of the center-radial pores, the position of the peak of DMSNs-epoxy remains at 21 nm because of the small molecular size of epoxy group. On the other hand, the position of mesopore peak slightly shifts to 19 nm for DMSNs-PEI, indicating the successful grafting of PEI (with larger molecular size) on the surface of center-radial large pore. After epoxy grafting and PEI modification, both the Brunauer–Emmett–Teller (BET) surface area and the total pore volume of DMSNs-epoxy and DMSNs-PEI decreased (Table 1), but the latter sample still possesses high BET surface area (>326 m^2 g^{-1}) and large total pore volume (>1.16 cm^3 g^{-1}) suitable for gene loading.

Solid state ^{13}C nuclear magnetic resonance (NMR) spectrum of DMSNs-PEI was obtained to elucidate the successful introduction of PEI to the DMSNs (Figure S2, Supporting Information). The broad peak between 65 and 80 ppm is assigned to the carbon connected with oxygen atom, and the broad peak between 40 and 60 ppm belongs to the carbon connected to nitrogen atom.[33,34] The chemical shifts at 8.8 and 23.4 ppm are attributed to the two other carbon atoms. These data indicate the successful introduction of PEI.[33,34] This was also confirmed by Fourier transform infrared spectroscopy (FTIR, Figure S3, Supporting Information), with the appearance of the absorption bands at 1465 cm^{-1} (C-N stretching) and at 2842 and 2932 cm^{-1},[13,30] and energy-dispersive X-ray (EDX, Figure S4, Supporting Information) spectra (the N amount was ca. 2.4 wt% in DMSNs-PEI).

The content of organics in DMSNs-epoxy and DMSNs-PEI was measured by thermogravimetric analysis (TGA) (Figure S5, Supporting Information). The weight loss from 200 to 700 °C are found to be 2.3 and 11.9% for DMSNs-epoxy and DMSNs-PEI, respectively, compared to the unmodified DMSNs-ext. These weight losses originate from the combustion of the organic components ($-C_3H_6OCH_2CHCH_2O$ and $-C_3H_6OCH_2CHCH_2O$-PEI) from the DMSNs. The surface coverage amounts of epoxy group and PEI could be calculated to be 0.20 and 0.13 mmol/g.

DMSNs-PEI can be well dispersed in water and no precipitation is observed after static storage for over one week, indicating that the surface PEI modification can sufficiently

Table 2. Hydrodynamic particle sizes and zeta (ζ) potentials of the different DMSNs dispersed in water at pH ≈ 7.4 and room temperature.

Sample name	Zeta potential (mV)	z-average particle size (nm)
DMSNs-ext	−25.8	171
DMSNs-epoxy	−29.6	174
DMSNs-PEI	+34.3	178
DMSNs-PEI@siRNA	−22.8	192
DMSNs-PEI@siRNA@AC-PEI	+28.2	218

enhance colloidal stability. The hydrodynamic size and zeta (ζ) potential values of DMSNs were measured using dynamic light scattering (Figure S6 and **Table 2**). The isoelectric point shifts from pH 3.2 (HPSNs-ext) to pH 9.6 (DMSNs-PEI) in water and the apparent average hydrodynamic particle size slightly increases from 171 nm (DMSNs-ext) to 178 nm (DMSNs-PEI), which could be attributed to the grafting of PEI.[11–16,35] These hydrodynamic particle sizes are larger than those observed from SEM and TEM, which is in line with the additional hydration of particle surface.[10,11]

2.2. Gene Loading Capability

The gene loading capability of DMSNs-PEI was examined by agarose gel electrophoresis using naked siRNA as a control. The DMSNs-PEI@siRNA complexes were prepared at varied weight ratios (the amount of siRNA was fixed at 0.2 μg) from 1/1 to 20/1. Based on the results in **Figure 3**a, the maximum siRNA binding capacity of DMSNs-PEI can be calculated to be ca. 158 μg siRNA/mg DMSNs-PEI, which corresponds to a much higher siRNA loading capacity compared to other previously reported silica-based gene carriers.[10–18] This high capacity possibly results from the increased surface positive charge density due to the introduction of PEI onto the unique center-radial pores of DMSNs-PEI. When the cell culture solution (DMEM with 10% FBS) was added, a partial (ca. 37%) siRNA escape from DMSNs-PEI could be observed (Figure 3b), and the released siRNA amount decreased with increasing DMSNs-PEI/siRNA weight ratio owing to a stronger electrostatic interaction at higher DMSNs-PEI/siRNA weight ratio. This finding suggests that either one or more compounds with negative charges in the cell culture medium exhibit preferential adsorption onto the DMSNs-PEI, thus a few siRNA may be

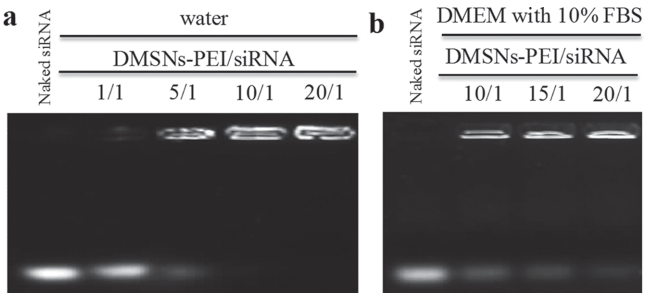

Figure 3. Agarose gel electrophoresis of DMSNs-PEI and siRNA at various weight ratios in a) water and b) DMEM with 10% FBS.

drawn out of the particles. This undesired siRNA leakage was also reported in previously developed silica-based gene carriers without additional polymer coating as a protection layer.[17,18] The specific amount of released siRNA is dependent on several factors, such as the density of modified positive charge, the pore size in the carriers, the weight ratios of carrier/siRNA, the concentrations of serum protein, and so on.

2.3. AC-PEI Coating

Polyethyleneimine (PEI) is one of the most popular cationic gene delivery carriers.[36,37] High molecular weight PEI, such as linear PEI with a molecular weight of 22 kDa (LPEI: 22K) or branched PEI with a molecular weight of 25 KDa (BPEI: 25K), exhibits excellent gene delivery capability, but it also demonstrates higher cytotoxicity due to their high positive charge density. In contrast, low molecular weight PEI, such as branched PEI with a molecular weight of 800 (PEI: 800) is non-cytotoxic, but it has a low gene binding capability. In the present study for efficient PEI coating, a non-toxic, biodegradable and autofluorescent AC-PEI[30,31] was specially designed. This AC-PEI can coat the surface of the gene-loaded particles by multipoint electrostatic interactions, which have been widely adopted for layer-by-layer polyelectrolyte self-assembly and particle assembly.[11,12,38–47] Furthermore, negatively charged gene molecules can be employed as a special biological polyanion for gene loading.[40,41] The AC-PEI coating on the surface of gene-loaded particles is expected to effectively inhibit gene leakage. The AC-PEI-coated delivery system should also display negligible cytotoxicity since AC-PEI can be biodegraded into low molecular weight PEI due to its response to endosomal acidic pH and cytoplasmic GSH in the intracellular microenvironment, thus effectively avoiding cytotoxicity caused by exogenous macromolecule accumulation. Moreover, the triggered gene release and AC-PEI degradation may be monitored by the fluctuation of fluorescence, which makes it possible to achieve traceable gene release in the absence of external fluorescence labelling.

Based on the result of agarose gel electrophoresis, siRNA is first loaded in the DMSNs-PEI according to different weight ratios of DMSNs-PEI/siRNA from 15/1 to 10/1 to 6/1. At the weight ratio of 10/1, the DMSNs-PEI@siRNA complexes were separated out from the solution by centrifugation. The siRNA concentration in the supernatant was almost negligible, and DMSNs-PEI@siRNA complexes in aqueous suspension demonstrate a negative charge of –22.8 mV and apparent hydrodynamic particle size of 192 nm (**Figure 4** and Table 2), which is suitable for subsequent AC-PEI coating. After AC-PEI coating on the surface of DMSNs-PEI@siRNA, DMSNs-PEI@siRNA@AC-PEI complexes in aqueous suspension have positive charge of +28.2 mV and hydrodynamic particle diameter of 218 nm (Figure 4 and Table 2). The average hydrodynamic particle size and zeta potential of DMSNs-PEI@siRNA@AC-PEI in DMEM

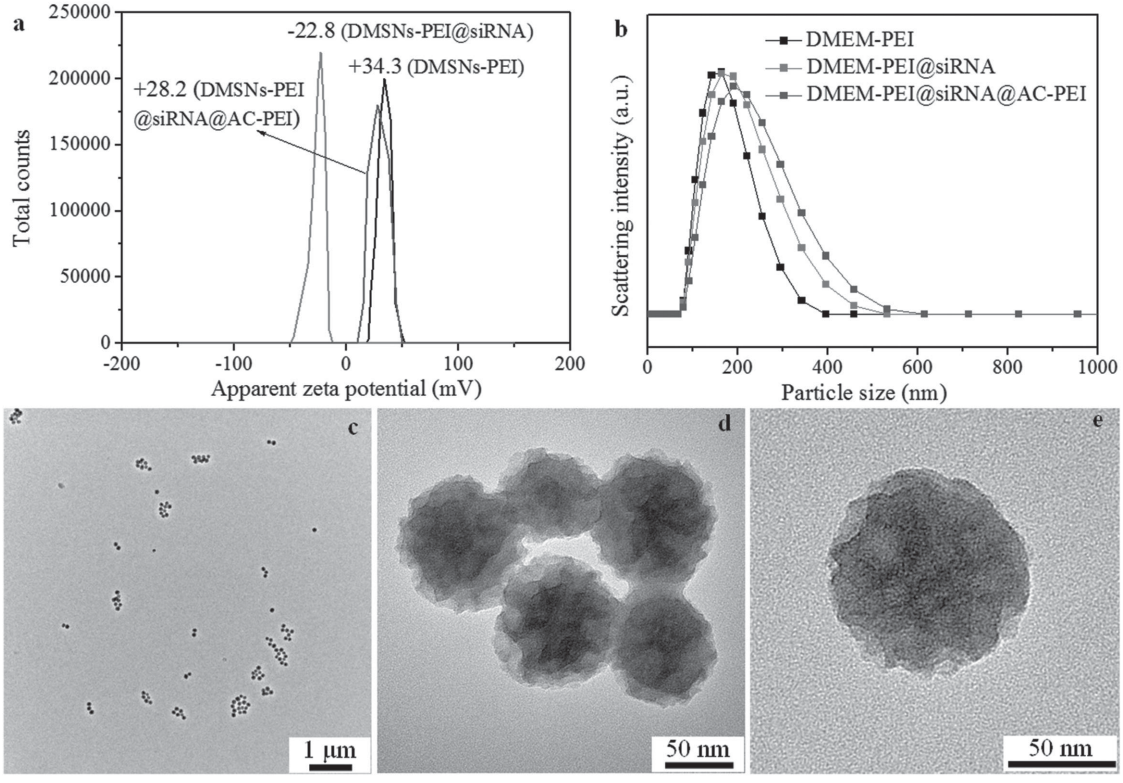

Figure 4. a) Zeta potentials and b) hydrodynamic particle sizes of DMSNs-PEI, DMSNs-PEI@siRNA, and DMSNs-PEI@siRNA@AC-PEI dispersed in water at pH ≈ 7.4 and room temperature. c–e) TEM images of the constructed gene delivery systems (DMSNs-PEI@siRNA@AC-PEI). The existence of some blurs on the particle surface indicates that polymers are successfully coated on the surface of DMSNs-PEI by electrostatic interactions.

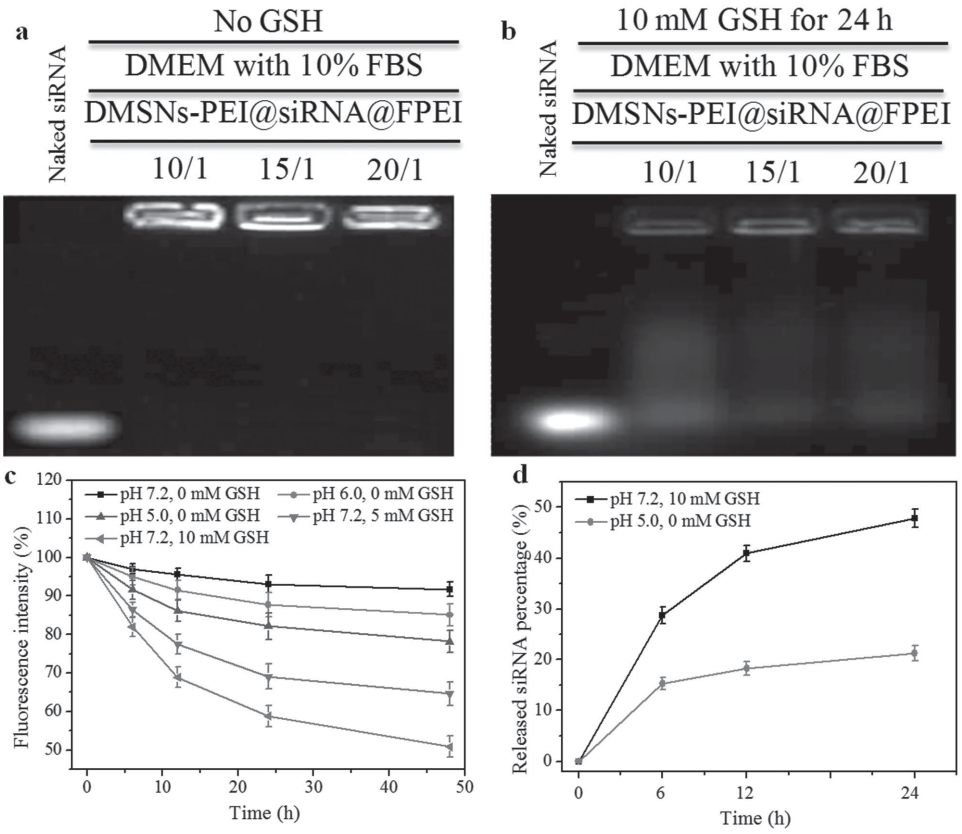

Figure 5. Agarose gel electrophoresis of DMSNs-PEI and siRNA at varied weight ratios after AC-PEI coating (i.e., DMSNs-PEI@siRNA@AC-PEI) a) without and b) with GSH in DMEM with 10% FBS. c) Time-dependence of the fluorescent intensity of the DMSNs-PEI@PAA@AC-PEI under various simulated conditions. d) siRNA release profiles from DMSNs-PEI@siRNA@AC-PEI under two simulated conditions.

containing 10% serum were estimated to be ca. 672 nm and –6.1 mV. The increased hydrodynamic size and the negative surface charge can be attributed to the adhesion of various proteins with negative charges in the medium.[18] The obvious size increase is undesired for in vivo applications. This has been a big and common disadvantage for most developed silica-based gene carriers,[10–18] which is expected to be overcome by PEGylation or zwitterionic modification on the particle surface.[48,49]

TEM images of DMSNs-PEI@siRNA@AC-PEI in Figure 4c–e show that the center-radial large pores are filled with some polymer, confirming that siRNA and AC-PEI are successfully coated on the surface of DMSNs-PEI. The slight yellow color (Figure S7, Supporting Information) and green fluorescence images (Figure S8, Supporting Information) of DMSNs-PEI@siRNA@AC-PEI complexes also evidence the successful coating of AC-PEI. The DMSNs-PEI@siRNA@AC-PEI complexes display fluorescent property with the maximum excitation and emission wavelengths at 462 and 488 nm, respectively, which are identical to the values of AC-PEI (Figure S9, Supporting Information). Moreover, after the AC-PEI is coated on the surface of DMSNs-PEI@siRNA, the result of agarose gel electrophoresis shows that no siRNA leakage is observed, indicating that the AC-PEI coating can efficiently stop siRNA leaching from the complexes into DMEM with 10% FBS (**Figure 5**a).

2.4. pH and GSH Responsive Property

To mimic intracellular microenvironment-responsive gene release from the DMSNs-PEI@siRNA@AC-PEI complexes, the GSH-triggered gene release process was investigated by agarose gel electrophoresis. GSH, which exists with huge concentration difference (100–1000 times) in intracellular (ca. 2–10 mM) and extracellular (ca. 2–10 μM) environments,[19,20,50–52] has been recognized as an ideal and ubiquitous stimulus inside cells to perform efficient intracellular-responsive drug release.[4,5] With 10 mM of GSH in DMEM with 10% FBS, long white bands (not white lines) are observed (Figure 5b), indicating that some siRNA molecules are released from DMSNs-PEI@siRNA@AC-PEI, and the released species should be complexes of siRNA and the short chain PEI.[53,54] The binding interaction between the low molecular weight PEI and siRNA is very weak, which can facilitate further release of free siRNA. Also, the released siRNA amount decreases with increasing DMSNs-PEI/siRNA weight ratio owing to stronger electrostatic interactions at higher DMSNs-PEI/siRNA weight ratio. Due to cleavage of the disulfide bonds of AC-PEI in the presence of GSH, the AC-PEI network structures collapse and molecules can be exchanged between siRNA and the negatively charged compounds in the cell culture medium. Furthermore, because of the existence of many negatively charged macromolecules in the cytoplasm, it is reasonable to speculate that the loaded gene cargoes can be controllably released from

the DMSNs-PEI@siRNA@AC-PEI complexes after cell uptake, using the trigger of intracellular reductive GSH.[19,20,30,31,50–52]

To further investigate the intracellular microenvironment-responsiveness on the fluorescence and gene release of the DMSNs-PEI@siRNA@AC-PEI complexes, DMSNs-PEI@siRNA@AC-PEI complexes were incubated in various simulated in vivo conditions including the physiological microenvironment in blood plasma (reductive agent free, pH 7.2), the late endosome (reductive agent free, pH 5.0) and the cytoplasm (2–10 mM of reductive agent, pH 7.2). Due to the expensive price of siRNA, poly(acrylic acid) (PAA) with negative charge was used to replace siRNA to construct large amount of DMSNs-PEI@PAA@AC-PEI complexes (Table S1, Supporting Information) for studying the fluorescent properties of DMSNs-PEI@siRNA@AC-PEI. The fluorescence intensities of the DMSNs-PEI@PAA@AC-PEI complexes were monitored by fluorescence spectrophotometry, and the released siRNA amount from DMSNs-PEI@siRNA@AC-PEI was assessed at the same time based on agarose gel electrophoresis. The fluorescence intensity of the DMSNs-PEI@PAA@AC-PEI complexes is stable at pH 7.2, but slightly drops to 76% of the maximum fluorescence intensity in an acidic environment of pH 5.0 after 48 h incubation (Figure 5c). It can be observed that ca. 21% of the loaded siRNA is released from the complexes in the acidic environment (pH 5.0) (Figure 5d). The small decrease in fluorescence intensity results from the slight hydrolysis of the Schiff-base,[30,31,55] while the release of small siRNA amount may be due to the combined action of the slight hydrolysis of the Schiff-base and the partial protonation of phosphate groups in siRNA at lower pH. The cleavage of acetic acid from AC-PEI may form a few small interspaces, and the less negatively charged siRNA may reduce the electrostatic attraction between siRNA and AC-PEI,[41–43] thus resulting in the siRNA release by substitution with negatively charged compounds in the cell culture medium. This decrease of fluorescence intensity and the siRNA release can be mainly attributed to the degradation of AC-PEI network structures into small PEI because of GSH-triggered disulfide bonds cleavage.[19,20,30,31,50–52] Based on the data in Figures 5c and 5d, a simple and rough time-dependent quantitative correlation between the siRNA release and the decrease of fluorescence intensity can be given, as summarized in Figure S10, Supporting Information, which shows that the fluorescent intensity decreases about 42% with 10 mM of GSH (pH 7.2) together with about 48% release of the loaded siRNA after 24 h treatment. This correlation between siRNA release and fluorescence reduction provides a new opportunity to track gene release and AC-PEI biodegradation through the variation of the AC-PEI fluorescence.

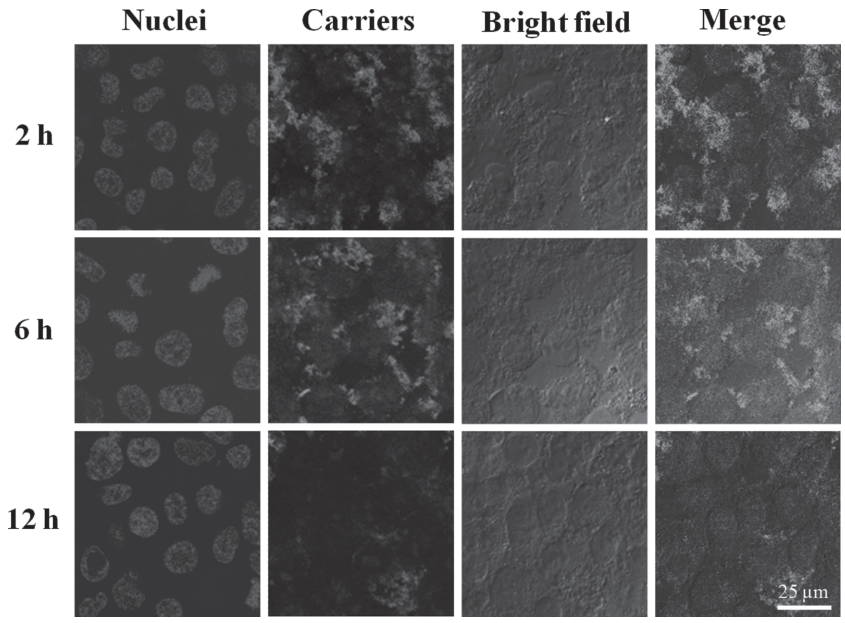

Figure 6. CLSM fluorescent images of cell uptake of DMSNs-PEI@PAA@AC-PEI complexes by KHOS cells at 2, 6 and 12 h. For 12 h observation, the complexes had been washed away and the cells were further incubated for 6 h.

2.5. Fluorescent Tracking in Vitro

The intracellular microenvironment-responsive behavior of DMSNs-PEI@PAA@AC-PEI complexes was monitored in osteosarcoma KHOS cells at different time intervals using confocal laser scanning microscopy (CLSM) and flow cytometry. As shown in **Figure 6**, after 2 h of incubation, many green fluorescent spots were observed on the surface of cell membrane, and a few green fluorescent spots can be monitored in the cells, indicating that some complexes have entered into cells through endocytosis. With further increase of the culture time from 2 to 6 h, the green fluorescent spots in the cells gradually increase. Interestingly, after the complexes were washed away from the cells at 6 h of incubation and the cells continue to incubate for 6 h, the green fluorescent spots become weaker in the cell interior than those after 6 h incubation, while a small number of green fluorescent spots on the surface of cell membrane are still bright. Flow cytometry results show that ca. 50% of cells contain the DMSNs-PEI@PAA@AC-PEI complexes at 2 h incubation, and the percentage increased to ca. 92% at 6 h and falls to ca. 30% after 12 h incubation (Figure S11, Supporting Information). For the incubation between 2 to 6 h, the increase of fluorescent green spots suggests cell uptake of more and more DMSNs-PEI@PAA@AC-PEI complexes. The observed decrease of fluorescence after 6 h is due to the hydrolysis of the Schiff-base in the late endosomes by a response to endosomal pH (c.a. 5.0–6.5) and the cleavage of disulfide bonds by response to the cytoplasmic GSH enzyme (2–10 mM). The above time-dependent fluorescent evolution is similar to that of AC-PEI alone as control (Figure S12) and the data in our previous reports.[30,31] The fluorescent brightness of DMSNs-PEI@PAA@AC-PEI in CLSM images is obviously higher than that of AC-PEI only (Figure 6 and S12), which may be the result from the fact that DMSNs-PEI@PAA@AC-PEI complexes in DMEM with 10% serum have larger particle sizes and higher cellular uptake than AC-PEI only.

These experimental results firmly establish that the fluorescence of DMSNs-PEI@PAA@AC-PEI complexes is responsive to the intracellular microenvironment. Since the loss of fluorescence for the DMSNs-PEI@PAA@AC-PEI complexes is directly correlated to the gene release (Figure 5c,d), the AC-PEI can be used to monitor pH- and GSH-responsive gene release processes. Evidently, the AC-PEI coating permits tracking the gene transport and the release process in vitro through monitoring the fluorescence of DMSNs-PEI@siRNA@AC-PEI complexes.

2.6. Cytotoxicity Study

The cytotoxicity of DMSNs-PEI and DMSNs-PEI@PAA@AC-PEI was evaluated by measuring the cell viability using 3-(4,5-dimethylthiazol-2-yl)-2,5-diphenyltetrazolium bromide (MTT) assays against osteosarcoma cell line KHOS cells in the typical concentration range (5–1000 μg/mL) for the delivery system (**Figure 7**a). PAA is used to replace the siRNA to investigate the cytotoxicity of the resultant delivery system without siRNA loading. The cytotoxicity slightly increased as the particle concentration increases. After 24 h of incubation, the average cell viabilities of three cell lines are above 80%, even at a high concentration of 1000 μg particles/mL in the cell culture solution, while the average cell viability in the case of branched 25 kDa PEI decreases to about 36% at the concentration of 100 μg/mL in the cell culture medium (Figure 7a). Therefore, the DMSNs-PEI and DMSNs-PEI@PAA@AC-PEI show low cytotoxicity and can be considered as safe nanocarriers compared with commercial 25 kDa branched PEI, which is in line with our previous results.[13,30,31]

2.7. Biological Function Assay in Delivering Functional siRNA to Cells

To investigate whether the DMSNs-PEI@siRNA@AC-PEI delivery system could efficiently deliver biofunctional siRNA into cells for gene therapeutic applications, DMSNs-PEI@siRNA system was used as contrast, and the siRNA against polo-like kinase 1 (PLK1) was chosen and tested for gene silencing effect in osteosarcoma cell line KHOS cells. The oncogenic gene is highly expressed in osteosarcoma cells, and the inhibition of PLK1 by siRNA can induce cell apoptosis.[14] The esiRNA1, which targets enhanced Green Fluorescent Protein (i.e., eGFP), was used as a negative control in KHOS cells lacking eGFP. As illustrated in Figure 7b, compared to the DMSNs-PEI@esiRNA1 control, DMSNs-PEI@PLK1 siRNA and DMSNs-PEI@PLK1 siRNA@AC-PEI can induce a noticeable decrease of cell viability, and the increase of DMSNs-PEI@PLK1 siRNA and DMSNs-PEI@PLK1 siRNA@AC-PEI concentrations can result in a little higher decrease of cell viability. However, although the increase in their concentrations is large, their induced decrease of cell viability is limited, which is similar to some previously reported results.[13,14,16] The specific reason for this behavior is, however, still unclear. Moveover, DMSNs-PEI@PLK1 siRNA@AC-PEI causes higher reduction (15–20%) of cell viability (i.e., better gene silencing effect)

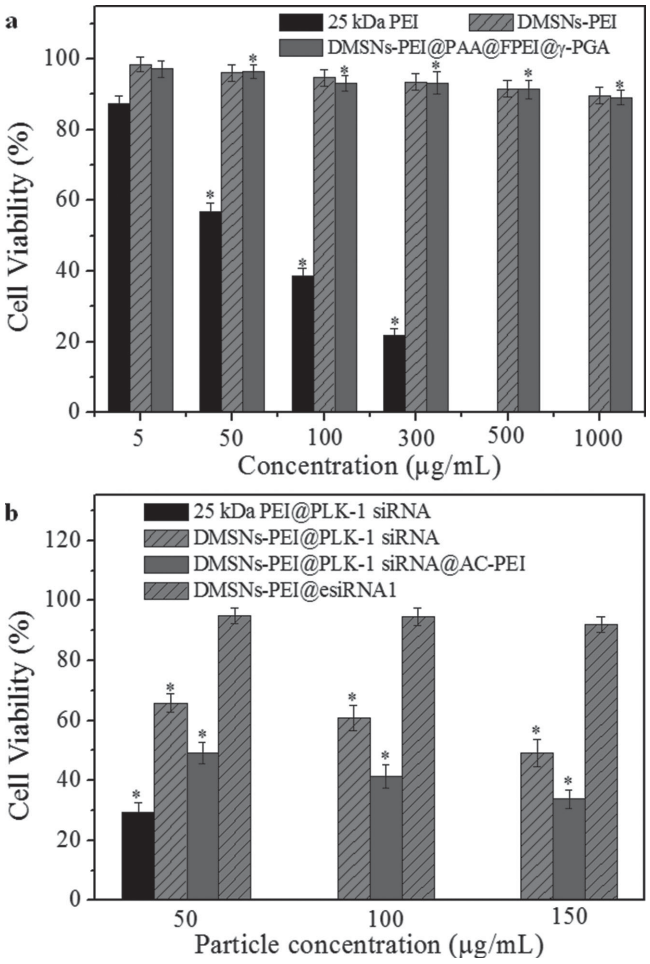

Figure 7. a) Cytotoxicity of 25 kD branched PEI, DMSNs-PEI and DMSNs-PEI@PAA@AC-PEI against KHOS cells. b) Biological function analysis of DMSNs-PEI delivery systems by delivering functional siRNAs against oncogenes PLK1 that are over-expressed in osteosarcoma cell line KHOS. The DMSNs-PEI were loaded with siRNA at the fixed weight ratio of 10:1. The DMSNs-PEI@siRNA with and without AC-PEI coating were incubated with KHOS for 48 h under varied particle concentration of 50, 100 and 150 μg/mL, and thus, the corresponding siRNA concentrations are 5, 10 and 15 μg/mL. The esiRNA1 was used as a negative control. Positive control was the cells without siRNA and particle treatment and regarded as 100% viable. Each data point in (a) and (b) represents the mean + SD (standard deviation) of 3 replicate experiments. One-tailed and unpaired Student's t-test was used to test the statistical significance of the differences. One way analysis of variance was used when more than two groups were compared with a single control. A value of $p < 0.05$ is considered to be significant. *$p < 0.05$.

than DMSNs-PEI@PLK1 siRNA. DMSNs-PEI@PLK1 siRNA@AC-PEI achieve ca. 70% reduction of cell viability at the concentration of 150 μg/mL, and this gene silencing capability is considerably high and even better than 25 kDa branched PEI (ca. 29% = 57% – 28% at the concentration of 50 μg/mL), and commercially available gene transfection reagent, Lipofectamine 2000 (ca. 65% according to the manufacturer's protocol). The high gene silencing capability of DMSNs-PEI@PLK1 siRNA@AC-PEI may be due to a combination of no gene leakage, efficient cellular uptake and the intracellular microenvironment-responsive siRNA release.

3. Conclusions

In summary, we have successfully developed a novel intracellular microenvironment-sensitive fluorescence label-free nanostructured dendrimer-like nanocarrier for traceable, effective and safe gene delivery. The developed nanocarriers have high gene loading capacity and low cytotoxicity owing to their center-radial pore structure together with smart surface modification and functionalization. The coating of autofluorescent and biodegradable AC-PEI on the gene-loaded particle effectively stops gene leakage from the carrier. Moreover, the stimuli-responsive fluorescent and degradable properties of AC-PEI toward endosomal acidic pH and cytoplasmic GSH not only can achieve controlled gene release, but also allow monitoring the gene delivery and release profiles in the absence of external fluorescence labelling. These results show that DMSNs-PEI@gene@AC-PEI delivery system is very promising for gene therapeutic applications. In addition, by layer-by-layer electrostatic assembly, other molecules (such as hyaluronic acid) may be adsorbed on the particle surface in order to improve the colloidal stability and achieve targeting delivery.

4. Experimental Section

Chemicals: Fetal bovine serum (FBS), phosphate buffered saline (PBS), Hoechst 33258 and 0.25% (w/v) trypsin-0.03% (w/v) ethylenediaminetetraacetic acid (EDTA) solution were purchased from Gibco-BRL (Grand Island, U.S.A.). Gel Red (10000x in water) was purchased from Biotium, Australia. Gel loading dye blue (6x) was purchased from Biolab, Australia. Dialysis bag (12–14 kDa) was purchased fromSpectra Labs. KHOS (human osteogenic sarcoma) cell lines, polo-like-kinase (PLK-1) siRNA (siRNA sequences are PLK-S, 5′-CCAUUAACGAGCUGCUUAATT-3′; PLK-AS, 5′-UUAAGCAGCUCGUUAAUGGTT-3′), esiRNA targeting enhanced Green Fluorescent Protein (esiRNA1), 3-(4,5-dimethylthiazol-2-yl)-2,5-diphenyltetrazolium bromide (MTT), L-Glutathione reduced (GSH, ≥ 98%), tetraethyl orthosilicate (TEOS, ≥98%), DL-Dithiothreitol (DTT, ≥98%), (3-Glycidyloxypropyl)trimethoxysilane (3-GPS, ≥98%), cetyltrimethylammonium tosylate (CTATos, ≥98%), Tris Acetate-EDTA (TAE) buffer (40 mM Tris-HCl, 1 v/v% acetic acid, and 1 mM EDTA), 1-ethyl-3-(3-dimethylaminopropyl) carbodiimide hydrochloride (EDC), N-hydroxysuccinimide (NHS), poly(acrylic acid) (PAA, M.W. = ~5000, 50 wt.% in H_2O), branched polyethylenimine (PEI, M.W. = 0.8 kDa and 25 kDa PEI), Dulbecco's modified eagle medium (DMEM), aqueous ammonia (NH_4OH, 30%), hydrochloric acid (HCl, 37%), triethanolamine (TEA), acetaldehyde, formaldehyde, dimethyl sulfoxide (DMSO) and other chemicals not mentioned were purchased from Sigma Aldrich. All materials were of analytical grade and used as received without further purification. Millipore water from a three-stage Millipore Mill-Q Plus 185 purification system (Academic) with a resistivity higher than 18.2 MΩ·cm was used in all experiments.

Characterizations: Scanning electron microscopy (SEM) observations were carried out on a FEI Quanta 450 FEG environmental emission scanning electron microscope operated at 10 kV. Specimens were coated with a layer of platinum by ion sputtering before SEM observations. For transmission electron microscopy (TEM) observations, the powder products were dispersed in ethanol by sonication for 10 min, and added on carbon-coated copper grids. TEM observations were carried out on a FEI Tecnai G2 Spirit transmission electron microscope at an acceleration voltage of 120 kV. UV–Vis absorption spectra were recorded on a UV-2600 spectrophotometer (Shimadzu Corporation). Fluorescent emission and excitation spectra were recorded on a RF-5301PC Spectrofluorophotometer (Shimadzu Scientific Instruments). Fourier transform infrared (FTIR) spectra of the samples were recorded on a Thermo Scientific NICOLET 6700 FTIR spectrometer at room temperature. Thermogravimetric analysis (TGA) of samples was performed on a S60/51920 TGA/DSC thermogravimetric analyzer from Setaram Instrumentation, using an oxidant atmosphere (oxygen, 30 mL/min) with a heating rate of 10 °C/min from room temperature to 800 °C. Nitrogen adsorption-desorption measurements were carried out at –196 °C using the volumetric method on a TriStar II surface area and porosity analyzer from Micromeritics. Prior to the measurement, the products were degassed at 120 °C for at least 6 h. Brunauer-Emmett-Teller (BET) specific surface areas were calculated by using adsorption data at a relative pressure range of P/P_0 range of 0.05–0.25. Pore size distributions were estimated from adsorption branch of the isotherm using the Barrett-Joyner-Halenda (BJH) method. Pore volumes were determined from the amounts of N_2 adsorbed at the single point of $P/P_0 = 0.99$. The particle sizes and zeta-potentials of varied nanoparticles and complexes were measured using a Malvern Zetasizer Nano ZS (Malvern Inst. Ltd., U.K.) equipped with four-side clear cuvettes or the ZET 5104 cell at room temperature. ^{13}C solid state cross-polarization magic-angle spinning nuclear magnetic resonance (^{13}C CP/MAS NMR) measurements were performed on a Bruker Avance III 400 Mhz spectrometer equiped with a 7mm solid state probe. Sample was spun at 2.5kHz. CP/MAS was carried out with a 2ms mixing time that was varied according the ramp Bruker program. Spectral width was 250 ppm, acquisition time 30ms, recycle delay 5s. Processed with line broadening = 25.

Synthesis of DMSNs: DMSNs were synthesized according to a reported method.[32] A typical synthesis was performed as follows: A mixture of cetyltrimethylammonium tosylate (CTATos, 0.96 g), triethanolamine (TEA, 0.1735 g) and water (50 mL) was stirred at 80 °C for 1 hour, and then TEOS (7.8 mL) was quickly added into the surfactant solution. The final mixture had the molar composition: 1.0SiO_2:0.06CTATos:0.026TEA:80.0H_2O. The mixture was stirred at 80 °C with a stirring speed of 1000 rpm for another 2 hours. The synthesized DMSNs were filtered, washed, and dried in the oven at 60 °C. The CTATos was removed from particles by template extraction. The as-prepared DMSNs (500 mg) was added into ethanolic HCl (conc. HCl (15 mL) in ethanol (100 mL)), and sonicated for 2 h. The suspension was stirred at 70 °C for 24 h. The extraction procedure was repeated thrice to efficiently remove the surfactant. Finally, the precipitates were centrifuged, washed with pure water, and dispersed in water or dried in air at 60 °C.

Epoxysilane Functionalization for DMSNs-Epoxy: DMSNs (200 mg) was added into toluene (30 mL). The mixture was first sonicated to facilitate particle dispersion, then 3-GPS (0.3 mL) was added. After stirred for 10 min at room temperature, the mixture was refluxed at 80 °C for 24 h. The solid product (DMSNs-epoxy) was centrifuged, washed with toluene, ethanol and water for three times, and dispersed in water or dried in air at 60 °C.

PEI Functionalization for DMSNs-PEI: DMSNs-epoxy (100 mg) was dispersed in water (30 mL), and sonicated to facilitate particle dispersion. PEI solution (0.4 mL, 100 mg/mL) was added into the dispersion. The formed mixture (pH: ca. 9.6) was stirred at room temperature for 12 h. At the final stage, ethylenediamine (20 µL) was added into the above mixture and stirred at room temperature for 6 h to block unreacted epoxy groups. The solid product (DMSNs-PEI) was centrifuged, washed with water for three times, and dispersed in water or dried in air at 60 °C.

Synthesis of AC-PEI: The acetaldehyde-modified-cystine (AC) was first synthesized by the reaction of acetaldehyde and cystine at room temperature.[30,31] L-cystine (1 g, 4.17 mmol) was dissolved in deionized water (50 mL), adjusted pH to 10 using NaOH solution (0.1 M) and incubated at 65 °C overnight. After cooled to room temperature, excessive acetaldehyde was dropwise added to the L-cystine solution over a 5 min period. The reaction mixture was stirred at room temperature for overnight. After that, the pH of solution was adjusted to pH 7 with HCl solution (0.1 M) and the solution was centrifuged at 16000 rpm for 10 min three times to remove the un-dissolved species. The supernatant

was collected and condensed using a rotary evaporator. The AC powder was finally obtained by freeze-drying under vacuum. Subsequently, AC molecule was employed to crosslink non-toxic low molecular weight branched PEI (M.W.: 800 Da) into higher molecular weight PEI by EDC/NHS chemistry. In a typical procedure, AC (20 mg), EDC (100 mg) and NHS (120 mg) was dissolved into water (20 mL), and the pH of the formed solution was adjusted to be ca. 7.2 by using NaOH solution (0.1 M) and stirred at room temperature for 30 min. Short branched PEI (100 mg) was dissolved in water (2 mL) and the pH of the PEI solution was adjusted to be ca. 7.2 by using HCl solution (0.1 M). PEI solution was then added to the activated AC solution and stirred in darkness at room temperature for 16 h. The reaction mixture was dialyzed against water in a dialysis membrane (molecular weight cut off 12–14 kDa, Merck) for four days, and the water was changed twice in one day during dialysis procedure. Finally, the solution in the dialysis membrane was collected and lyophilized to obtain the AC-crosslinked PEI (AC-PEI).

Binding of DMSNs-PEI and siRNA: The binding capability of siRNA to DMSNs-PEI was evaluated by agarose gel electrophoresis using naked siRNA as the control. Samples were prepared by mixing DMSNs-PEI and siRNA (0.2 μg) at different mixing weight ratios from 1:1 to 20:1 (DMSNs-PEI to siRNA). Gel loading dye blue was added in every sample. Following incubation for 30 min, the DMSNs-PEI@siRNA complexes were electrophoresed through a 0.8% agarose gel containing gel red in TAE buffer solution at 90 V for 30 min. The resulting siRNA migration patterns were recorded under UV irradiation (G-BOX, SYNGENE).

The Coating of AC-PEI: AC-PEI (polycation) was coated on the surface of gene-loaded DMSNs-PEI with negative charge by electrostatic interactions. Based on the result of agarose gel electrophoresis, siRNA was first loaded in the DMSNs-PEI according to varied weight ratio of DMSNs-PEI/siRNA from 15/1 to 10/1 to 6/1. At the weight ratio of 10/1, the DMSNs-PEI@siRNA complexes were separated out from solution by centrifugation. The siRNA concentration in supernatant was almost negligible, and DMSNs-PEI@siRNA complexes had negative charge and small apparent z-average hydrodynamic particle sizes. Thus, the weight ratio of DMSNs-PEI:siRNA was chosen to be 10:1. To perform AC-PEI coating on the surface of DMSNs-PEI@siRNA, AC-PEI solution (2 μL, 10 mg/mL) was added into DMSNs-PEI@siRNA aqueous suspension (0.2 mL, 0.5 mg/mL). After the mixture was stirred for 1 h, the AC-PEI-coated particles (DMSNs-PEI@siRNA@AC-PEI) were obtained by centrifugation and slightly washed with water. Due to the expensive price of siRNA, PAA with negative charge was used to replace siRNA to construct the large amount of DMSNs-PEI@PAA@AC-PEI complexes for investigating the fluorescent properties of DMSNs-PEI@siRNA@AC-PEI. The procedures of DMSNs-PEI@PAA@AC-PEI were the same as those of DMSNs-PEI@siRNA@AC-PEI except the use of PAA (to replace siRNA) and higher dosage.

GSH-Triggered Gene Release: The effects of the cell culture solution (DMEM with 10% FBS), AC-PEI coating on the surface of DMSNs-PEI@siRNA and GSH were investigated for the binding between DMSNs-PEI and siRNA by agarose gel electrophoresis using naked siRNA as the control. Samples were prepared by mixing DMSNs-PEI and siRNA (0.2 μg) at different mixing weight ratios from 10:1 to 20:1 (DMSNs-PEI to siRNA), and subsequently coated with AC-PEI. Control samples were prepared without AC-PEI coating. DMEM with 10% FBS (6 μL) was added into samples, which was incubated for 1 h. For GSH effect, DMEM with 10 mM GSH and 10% FBS (12 μL) was added into samples, which was incubated for 24 h. The sample complexes were electrophoresed through a 0.8% agarose gel containing gel red in TAE buffer solution at 90 V for 30 min. The resulting siRNA migration patterns were recorded under UV irradiation (G-BOX, SYNGENE).

pH- and GSH-Responsive Properties: To investigate pH effects, PBS solutions with varied pH values of 5.0, 6.0 and 7.2 were used. To study GSH effects, solutions (pH 7.2) with GSH concentrations of 0, 5 and 10 mM were used. DMSNs-PEI@PAA@AC-PEI complexes were first suspended in the above solutions to form a concentration of 0.5 mg mL^{-1} and stirred at 37 °C. Suspensions were directly taken at different time intervals, and their fluorescent intensity was recorded by a Shimadzu fluorescent spectrometer. After each measurement, the measured suspensions were put back into the previous suspensions to eliminate volume change.

Cytotoxicity of the Particles: Cell viability was determined using MTT assay following standard protocol. 25 kDa PEI solution, DMSNs-PEI and DMSNs-PEI@PAA@AC-PEI suspensions containing different concentrations (5–1000 μg/mL) were prepared in DMEM with 10% FBS. KHOS cells were inoculated and cultured in DMEM with 10% FBS in 96-well plates (200 μL medium/well) at a density of 1.0×10^5 cells/mL. After the cells were allowed to adhere overnight at 37 °C in a humidified atmosphere containing 5% CO_2, the growth media were replaced with fresh medium (200 μL) containing 25 kDa PEI, DMSNs-PEI and DMSNs-PEI@PAA@AC-PEI. Then, after cells were further incubated for 24 h, MTT (10 μL, 5.0 mg/mL in PBS) was added to each well, and cells were finally incubated for an additional 4.0 h at 37 °C. Subsequently, the growth medium was removed and DMSO (150 μL) was put into each well to make sure complete solubilization of formazan crystals. Finally, the absorbance was measured employing the Biotek Microplate Reader (Biotek, USA) at a wavelength of 595 nm. Data were expressed as mean ± standard deviation (SD) of at least three independent experiments.

Real-Time Tracking of DMSNs-PEI@PAA@AC-PEI Complexes In Vitro Khos Cells by Confocal Laser Scanning Microscopy and Flow Cytometry: The gene delivery process of DMSNs-PEI to transport siRNA into the KHOS cell was evaluated and tracked by the evolution of fluorescent intensity using the confocal laser scanning microscope. The KHOS cells were seeded at a concentration of 2×10^5 cells/well into 6-well plates loaded with cover-glass slides in 25 mm diameter and cultured in cell culture medium (DMEM supplied with 10% FBS, 2 mL) for 24 h. KHOS cells were incubated with fresh medium (2 mL) containing DMSNs-PEI@PAA@AC-PEI complexes (0.2 mg/mL) for 2 and 6 h, respectively, and then washed with PBS three times to remove the complexes. The cells, from which the complexes have been washed away at 6 h, were further incubated for 6 h to achieve the incubation of total 12 h. Subsequently, these cells were fixed with formaldehyde (1 mL, 4 wt.%). The cell membrane and nucleus were stained with Alexa Fluor 594 (100 μL, 5.0 μg/mL) and Hoechst 33258 (100 μL, 2 μM) for 10 min at room temperature, the cells were washed with PBS for three times and incubated with PBS (200 μL). The fluorescent images were observed by a CLSM (Leica Confocal 1P/FCS) equipped with a 405 nm diode laser for Hoechst 33258, a 460 nm argon ion laser for AC-PEI and a 561 diode laser for Alexa Fluor 594. High-magnification images were obtained with 100 × objective. Optical sections were averaged 4 times to reduce noise. Images were processed using Leica confocal software. On the other hand, the green fluorescence intensity of DMSNs-PEI@PAA@AC-PEI complexes was detected directly by a FACSCalibur flow cytometry (Becton Dickinson), and the percentages of these complexes in cells and on the cell surface were calculated by using normal cultured cell without complexes as the negative control. Briefly, cells were harvested by the digestion of trypsin after 2, 6 or 12 h incubation. 1×10^6 cells were washed with 2% FCS/PBS buffer, and centrifuged at 1000 rpm for 5 min. The cells were stained by propidium iodide in 1× PBS (400 mL, 0.5 mg/mL). Approximately $1–2 \times 10^4$ cells were analyzed at the rate of 200–600 cells per second. Cell Quest 3.3 software was used for data analysis.

Biological Function Assay for Delivering Functional siRNA: To examine whether the gene delivery system (DMSNs-PEI@siRNA@AC-PEI) can deliver functional molecules to cells for therapy, the polo-like-kinase (PLK-1) siRNA was chosen as a model functional therapeutic gene to test against KHOS cell line.[14] The esiRNA1, which targets enhanced Green Fluorescent Protein (i.e., eGFP), was used as a negative control in KHOS cells lacking eGFP. 25 kDa PEI was used as the positive control. Briefly, the KHOS cells were seeded in 96-well plate at a concentration of 1.0×10^5 cells/well in cell culture medium (200 μL). After inoculation, the cells were allowed to adhere overnight at 37 °C in a humidified 5% CO_2-containing atmosphere. KHOS cells were incubated with 25 kDa PEI@siRNA, DMSNs-PEI@siRNA or DMSNs-PEI@siRNA@AC-PEI at varied particle concentration of 50, 100 and 150 μg/mL (the weight ratio of DMSNs-PEI/siRNA was fixed at 10:1) for 48 h. MTT assays were used to assess their cell viabilities.

Supporting Information

Supporting Information is available from the Wiley Online Library or from the author.

Acknowledgements

This work was financially supported by the Australian Research Council (ARC) Discovery Projects (DP140104062, DP130104459, and DP110102877).

Received: July 18, 2014
Revised: September 17, 2014
Published online: October 6, 2014

[1] I. M. Verma, N. Somia, *Nature* **1997**, *389*, 239.
[2] I. M. Verma, M. D. Weitzman, *Annu. Rev. Biochem.* **2005**, *74*, 711.
[3] A. Fougerolles, H. P. Vornlocher, J. Maraganore, J. Lieberman, *Nat. Rev. Drug Discov.* **2007**, *6*, 443.
[4] M. A. Kay, J. C. Glorioso, L. Naldini, *Nat. Med.* **2001**, *7*, 33.
[5] S. D. Li, L. Huang, *Gene Ther.* **2006**, *13*, 1313.
[6] C. Hom, J. Lu, F. Tamanoi, *J. Mater. Chem.* **2009**, *19*, 6308.
[7] V. Mamaeva, C. Sahlgren, M. Lindén, *Adv. Drug Delivery Rev.* **2013**, *65*, 689.
[8] I. I. Slowing, J. L. Vivero-Escoto, C. W. Wu, V. S. Y. Lin, *Adv. Drug Delivery Rev.* **2008**, *60*, 1278.
[9] Y. Niu, A. Popat, M. Yu, S. Karmakar, W. Gu, C. Yu, *Ther. Deliv.* **2012**, *3*, 1217.
[10] H. K. Na, M. H. Kim, K. Park, S. R. Ryoo, K. E. Lee, H. Jeon, R. Ryoo, C. Hyeon, D. H. Min, *Small* **2012**, *8*, 1752.
[11] T. Xia, M. Kovochich, M. Liong, H. Meng, S. Kabehie, S. George, J. I. Zink, A. E. Nel, *ACS Nano* **2009**, *3*, 3273.
[12] X. Ma, Y. Zhao, K. W. Ng, Y. Zhao, *Chem. Eur. J.* **2013**, *19*, 15593.
[13] X. Du, Y. Bing, J. Liang, J. Bi, S. Dai, S. Z. Qiao, *Adv. Mater.* **2013**, *25*, 5981.
[14] S. B. Hartono, W. Gu, F. Kleitz, J. Liu, L. He, A. P. J. Middelberg, C. Yu, G. Q. Lu, S. Z. Qiao, *ACS Nano* **2012**, *6*, 2104.
[15] D. R. Radu, C. Y. Lai, K. Jeftinija, E. W. Rowe, S. Jeftinija, V. S. Y. Lin, *J. Am. Chem. Soc.* **2004**, *126*, 13216.
[16] D. Lin, Q. Cheng, Q. Jiang, Y. Huang, Z. Yang, S. Han, Y. Zhao, S. Guo, Z. Liang, A. Dong, *Nanoscale* **2013**, *5*, 4291.
[17] J. L. Steinbacher, C. C. Landry, *Langmuir* **2014**, *30*, 4396.
[18] X. Lia, Q. R. Xie, J. Zhang, W. Xia, H. Gu, *Biomaterials* **2011**, *32*, 9546.
[19] R. Cheng, F. Feng, F. Meng, C. Deng, J. Feijen, Z. Zhong, *J. Controlled Release* **2011**, *152*, 2.
[20] D. Oupický, J. Li, *Macromol. Biosci.* **2014**, *14*, 908.
[21] D. W. Pack, A. S. Hoffman, S. Pun, P. S. Stayton, *Nat. Rev. Drug Discov.* **2005**, *4*, 581.
[22] H. Wei, L. R. Volpatti, D. L. Sellers, D. O. Maris, I. W. Andrews, A. S. Hemphill, L. W. Chan, D. S. H. Chu, P. J. Horner, S. H. Pun, *Angew. Chem. Int. Ed.* **2013**, *52*, 5377.
[23] L. Gu, L. M. Nusblat, N. Tishbi, S. C. Noble, C. M. Pinson, E. Mintzer, C. M. Roth, K. E. Uhrich, *J. Controlled Release* **2014**, *184*, 28.
[24] Q. He, Z. Zhang, Y. Gao, J. Shi, Y. Li, *Small* **2009**, *5*, 2722.
[25] F. Lu, S. H. Wu, Y. Hung, C. Y. Mou, *Small* **2009**, *5*, 1408.
[26] M. Wang, X. Li, Y. Ma, H. Gu, *Int. J. Pharm.* **2013**, *448*, 51.
[27] W. Wei, L. Y. Wang, L. Yuan, Q. Wei, X. D. Yang, Z. G. Su, G. H. Ma, *Adv. Funct. Mater.* **2007**, *17*, 3153.
[28] Y. Yang, Y. Jia, L. Gao, J. Fei, L. Dai, J. Zhao, J. Li, *Chem. Commun.* **2011**, *47*, 12167.
[29] Y. Jia, J. Fei, Y. Cui, Y. Yang, L. Gao, J. Li, *Chem. Commun.* **2011**, *47*, 1175.
[30] X. Du, B. Shi, Y. Tang, S. Dai, S. Z. Qiao, *Biomaterials* **2014**, *35*, 5580.
[31] B. Shi, H. Zhang, S. Z. Qiao, J. Bi, S. Dai, *Adv. Healthcare Mater.* **2014**, doi: 10.1002/adhm.201400187.
[32] K. Zhang, L. L. Xu, J. G. Jiang, N. Calin, K. F. Lam, S. J. Zhang, H. H. Wu, G. D. Wu, B. Albela, L. Bonneviot, P. Wu, *J. Am. Chem. Soc.* **2013**, *135*, 2427.
[33] J. A. A. Sales, A. G. S. Prado, C. Airoldi, *Polyhedron* **2002**, *21*, 2647.
[34] S. B. Hartono, M. Yu, W. Gu, J. Yang, E. Strounina, X. Wang, S. Z. Qiao, C. Yu, *Nanotechnology* **2014**, *25*, 055701.
[35] G. V. Franks, *J. Colloid Interface Sci.* **2002**, *249*, 44.
[36] T. Merdana, J. Kopeček, T. Kissel, *Adv. Drug Deliv. Rev.* **2002**, *54*, 715.
[37] M. Morille, C. Passirani, A. Vonarbourg, A. Clavreul, J. P. Benoit, *Biomaterials* **2008**, *29*, 3477.
[38] Y. Yan, M. Björnmalm, F. Caruso, *Chem. Mater.* **2014**, *26*, 452.
[39] W. Tong, X. Song, C. Gao, *Chem. Soc. Rev.* **2012**, *41*, 6103.
[40] M. Y. Lee, S. J. Park, K. Park, K. S. Kim, H. Lee, S. K. Hahn, *ACS Nano* **2011**, *5*, 6138.
[41] Z. J. Deng, S. W. Morton, E. Ben-Akiva, E. C. Dreaden, K. E. Shopsowitz, P. T. Hammond, *ACS Nano* **2013**, *7*, 9571.
[42] Y. Zhu, J. Shi, W. Shen, X. Dong, J. Feng, M. Ruan, Y. Li, *Angew. Chem. Int. Ed.* **2005**, *44*, 5083.
[43] W. Feng, X. Zhou, C. He, K. Qiu, W. Nie, L. Chen, H. Wang, X. Mo, Y. Zhang, *J. Mater. Chem. B* **2013**, *1*, 5886.
[44] W. Feng, W. Nie, C. He, X. Zhou, L. Chen, K. Qiu, W. Wang, Z. Yin, *ACS Appl. Mater. Interfaces* **2014**, *6*, 8447.
[45] Y. Wang, Y. Yan, J. Cui, L. Hosta-Rigau, J. K. Heath, E. C. Nice, F. Caruso, *Adv. Mater.* **2010**, *22*, 4293.
[46] F. Caruso, R. A. Caruso, H. Möhwald, *Science* **1998**, *282*, 1111.
[47] X. Liu, X. Du, J. He, *Chem Phys Chem* **2008**, *9*, 305.
[48] G. Y. Tonga, K. Saha, V. M. Rotello, *Adv. Mater.* **2014**, *26*, 359.
[49] K. P. García, K. Zarschler, L. Barbaro, J. A. Barreto, W. Malley, L. Spiccia, H. Stephan, B. Graham, *Small* **2014**, *10*, 2516.
[50] M. H. Lee, Z. Yang, C. W. Lim, Y. H. Lee, S. Dongbang, C. Kang, J. S. Kim, *Chem. Rev.* **2013**, *113*, 5071.
[51] X. Ma, K. T. Nguyen, P. Borah, C. Y. Ang, Y. Zhao, *Adv. Healthcare Mater.* **2012**, *1*, 690.
[52] Y. Yan, Y. J. Wang, J. K. Heath, E. C. Nice, F. Caruso, *Adv. Mater.* **2011**, *23*, 3916.
[53] Y. Wang, P. Chen, J. Shen, *Biomaterials* **2006**, *27*, 5292.
[54] Q. Peng, Z. Zhong, R. Zhuo, *Bioconjugate Chem.* **2008**, *19*, 499.
[55] Y. Xin, J. Yuan, *Polym. Chem.* **2012**, *3*, 3045.